Published in final edited form as:

Bioconjug Chem. 2015 March 18; 26(3): 435–442. doi:10.1021/acs.bioconjchem.5b00089.

Improved Metabolic Stability for ^{18}F PET Probes Rapidly Constructed via Tetrazine *trans*-Cyclooctene Ligation

Ramajeyam Selvaraj[1,#], **Benjamin Giglio**[2,#], **Shuanglong Liu**[3,#], **Hui Wang**[2], **Mengzhe Wang**[2], **Hong Yuan**[2], **Srinivasa R. Chintala**[1], **Li-Peng Yap**[3], **Peter S. Conti**[3], **Joseph M. Fox**[1,*], and **Zibo Li**[2,*]

[1]Brown Laboratories, Department of Chemistry and Biochemistry, University of Delaware, Newark, DE 19803, USA

[2]Department of Radiology and Biomedical Research Imaging Center, University of North Carolina at Chapel Hill, Chapel Hill, NC 27599, USA

[3]Molecular Imaging Center, Department of Radiology, University of Southern California, Los Angeles, CA90033, USA

Abstract

The fast kinetics and bioorthogonal nature of the tetrazine *trans*-cyclooctene (TCO) ligation makes it a unique tool for PET probe construction. In this study, we report the development of an ^{18}F-labeling system based on a CF_3-substituted diphenyl-*s*-tetrazine derivative with the aim of maintaining high reactivity while increasing *in vivo* stability. c(RGDyK) was tagged by a CF_3-substituted diphenyl-*s*-tetrazine derivative via EDC-mediated coupling. The resulting tetrazine-RGD conjugate was combined with a ^{19}F-labeled TCO derivative to give HPLC standards. The analogous ^{18}F-labeled TCO derivative was combined with the diphenyl-*s*-tetrazine-RGD at μM concentration. The resulting tracer was subjected to *in vivo* metabolic stability assessment, and microPET studies in murine U87MG xenograft models. The diphenyl-*s*-tetrazine-RGD combines with an ^{18}F-labeled TCO in high yields (>97% decay-corrected on the basis of TCO) using only 4 equiv of tetrazine-RGD relative to the ^{18}F-labeled TCO (concentration calculated based on product's specific activity). The radiochemical purity of the ^{18}F-RGD peptides was >95% and the specific activity was 111 GBq/μmol. Noninvasive microPET experiments demonstrated that ^{18}F-RGD had integrin-specific tumor uptake in subcutaneous U87MG glioma. *In vivo* metabolic stability of ^{18}F-RGD in blood, urine and major organs showed two major peaks: one corresponded to the Diels-Alder conjugate and the other was identified as the aromatized analog. A CF_3-substituted diphenyl-*s*-tetrazine displays excellent speed and efficiency in ^{18}F-PET probe construction, providing nearly quantitative ^{18}F labeling within minutes at low micromolar concentrations. The resulting conjugates display improved *in vivo* metabolic stability relative to our previously described system.

Corresponding Authors: jmfox@udel.edu; ziboli@med.unc.edu.
[#]These authors contributed equally to the research work.

INTRODUCTION

Positron emission tomography (PET) is a powerful and highly sensitive imaging technology with the capacity to observe metabolic processes and track radiolabeled biomolecules *in vivo*.[1] Of the various positron emitting radionuclides, ^{18}F finds most extensive use due to its clinically attractive half-life ($t_{1/2}$ = 110 min) and high positron efficiency (β^+ = 99%). To date, clinical applications of PET have largely involved small molecule probes such as ^{18}F-2-deoxy-2-fluoroglucose.[2, 3] Currently, there is great interest in the development of peptidic and protein-based probes for ^{18}F PET imaging, with a correlated need to develop methods for bioligand probe construction. New methods for probe construction must operate efficiently within the constraints of ^{18}F-labeling chemistry, which include the limited nucleophilicity and short half-life of fluoride and the need to efficiently conjugate molecules at low concentrations relevant to radiochemical experimentation.

A variety of ^{18}F-labeled synthons have been developed and successfully applied to a host of peptides and proteins for ^{18}F-PET probe construction. The utility of many ^{18}F PET probes is hindered by multistep probe syntheses where ^{18}F is carried through multiple chemical intermediates—a major limitation given the technically demanding nature of ^{18}F radiochemistry. For the conjugation of ^{18}F to the biological ligand, peptides or proteins are often used in large excess in order to obtain reasonable yields for ^{18}F attachment. Additionally, ^{18}F-tagged proteins or large-peptides are often inseparable from their unlabeled precursors which can compromise the signal through competitive inhibition and result in low specific activity. Furthermore, sacrificing milligram quantities for labeling reactions is impractical for peptides or proteins that are not available in large quantity. Greatly needed are efficient and robust methods for labeling proteins and peptides by ^{18}F at low concentrations.

In 2008, we described methods for synthesizing *trans*-cyclooctene derivatives[4] and applying them in fast bioorthogonal reactions with tetrazines.[5] With strained TCO derivatives, rate constants of $k_2 > 10^6$ $M^{-1}s^{-1}$ have been measured.[6–9] Contemporaneous with the initial study of TCO, several groups described reactions of tetrazines with derivatives of norbornene[10] or the Reppe anhydride,[11] with a measured rate constant of $k_2 = 1.9$ $M^{-1}s^{-1}$ at 20 °C in PBS for norbornene conjugation. Recently, cyclopropenes,[12, 13] cyclooctynes,[6, 14, 15] and terminal alkenes[16] have also been used as dienophiles for tetrazine ligation. While each of these dienophiles offers complementary advantages, TCO derivatives display the fastest rate constants.

The tetrazine-TCO ligation has become broadly used for research in nuclear medicine including applications in pretargeted imaging,[17–19] and studies have been directed toward optimizing and improving the pharmacokinetics and pharmacodynamics for systems based on dipyridyl-*s*-tetrazine and monoaryltetrazines.[7, 17–25] In 2010, Robillard first showed that the tetrazine ligation method could be applied in a pre-targeted antibody using single photon emission computed tomography (SPECT).[23] More recently, Robillard has described factors that contribute to the *in vivo* stability of TCO's toward isomerization,[7] and clearing agents have been developed that improve tumor-to-blood (125 fold) ratios.[22] Weissleder has shown that polymer modified tetrazines can be used for *in vivo* bioorthogonal labeling and PET

imaging using an ^{18}F-labeled TCO derivative.[20] More recently, Weissleder and Lewis reported a pretargeting approach for PET imaging based on this method and demonstrated dramatically reduced nontargeted organ uptake.[24] Recently, the reaction of a ^{11}C-labeled tetrazine with a TCO derivative was described,[26] and Kuntner and Mikula described the development of a ^{18}F-labeled tetrazine with favorable pharmacokinetic properties.[25]

In 2010, we developed a radiolabeling method for bioconjugation based on the Diels-Alder reaction between dipyridyl-*s*-tetrazines and an ^{18}F-labeled *trans*-cyclooctene.[27] As shown in Figure 1, ^{18}F-labeled TCO **2** could be obtained in high radiochemical yield (71%) by combining nosylate **1** with ^{18}F-fluoride (100 mCi). ^{18}F-**2** is an effective reagent for creating ^{18}F-labeled probes within seconds at low micromolar concentrations, and we have used this reagent to make cyclic RGD (cRGD) and VEGF protein conjugates for cancer imaging[28, 29] and exendin-4 conjugates for applications in insulinoma imaging and diabetes monitoring.[30] Notably, these conjugates were synthesized without using a large excess of the peptidic labeling precursor (Figure 1b). Avoiding excess labeling precursor is critically important for proteins and large polypeptides such as exendin-4 (MW 4775), where the labeled and unlabeled peptide are not readily separable, and unlabeled peptide can significantly decrease signal due to competitive inhibition.[30] Weissleder and Lewis have also used ^{18}F-**2** in a number of applications including a recent demonstration of pretargeted imaging.[24]

An important factor that has not received significant attention is the metabolic stability of tetrazine-TCO conjugates. Dipyridyl-*s*-tetrazine-based probes with good pharmacokinetic properties have been constructed through conjugation to large peptides (exendin-4)[30] or by including PEG-spacers in antibody-pretargeting studies.[7, 22, 23] We also described that ^{18}F-*trans*-cyclooctene **2** undergoes very rapid conjugation with a dipyridyl-*s*-tetrazine-cRGD construct, and the resulting isomeric conjugates **4b** can be used to image tumors in mice (Fig. 1c). Here, a relatively high level of organ uptake in the liver and kidneys was observed, presumably due to the hydrophobic nature of the probe. Because of the high residence time in the liver, we expected that this system would provide a good platform to test and improve the metabolic stability of tetrazine-based probes. In our study on **4b**, an attempt to re-isolate radioactive **4b** from the major organs, urine and blood of a mouse was not unsuccessful, and only hydrophilic degradation products were observed by radio-HPLC analysis. We hypothesized that the imines of **4b**, flanked with electron withdrawing pyridines, may be susceptible to nucleophilic attack and thereby provide a possible handle for degradation. We also hypothesized that a conjugate (Fig 1d) with less electron withdrawing aromatic groups would be more stable. Here, we describe a 3,6-diphenyl-*s*-tetrazine derivative that displays fast conjugation rates toward ^{18}F-**2** and gives conjugates with improved metabolic stability in an *in vivo* mouse study. ^{18}F-labeling yields are discussed and the metabolic stability of the ^{18}F-**2** tagged cRGD conjugate is described. The PET probe was evaluated for integrin $\alpha_v\beta_3$ imaging in U87MG tumor-bearing mice by microPET.

RESULTS

Chemistry

The CF_3-substituted diphenyl-*s*-tetrazine **6**[35] was prepared by an improved two-step procedure and elaborated by EDC coupling to cRGD derivative **7** (Fig. 2a) To gauge the reactivity of derivatives of diaryltetrazine **6,** stopped flow kinetic analysis was used to measure the rate of the Diels-Alder reaction between tetrazine derivative **8** and equatorially substituted *trans*-cyclooctene derivative **9**, the precursor to ^{18}F-**2** (Fig. 2). The undecaethylene glycol sidechain of **8** was added to enhance water solubility. In water/MeOH (6:4, v/v) at 25 °C, a second order rate constant k_2 = 1000 ± 100 $M^{-1}s^{-1}$ was measured.

The cycloaddition reaction of tetrazine-cRGD **7** and ^{19}F-**2** provided ^{18}F-cRGD conjugates **10,** which were used as radiolabeling standards and for the integrin receptor binding assay. Consistent with the high reactivity of **8**, the pink color of tetrazine-cRGD **7** disappeared immediately upon mixing with ^{19}F-**2**. The identity of the ^{19}F-cRGD conjugates **10** were confirmed by LC-MS. As expected based from prior observation and a model study,[5, 9, 36] both aromatized conjugates **10b** were formed in addition to dihydropyridazine conjugates **10a** (Fig. 3a,b). Collectively, we refer to the mixture of aromatic and dihydropyridazine conjugates as **10**.

Radiochemistry

^{18}F-labeled *trans*-cyclooctene (^{18}F-**2**) was produced using the protocol developed in our laboratories,[27] and utilized in radiolabeling experiments with tetrazine-cRGD derivative **7** (Fig. 4). With only a 4-fold excess of **7** (4 μM) relative to ^{18}F-**2** (1 μM, calculated based on the specific activity of ^{18}F-**10a**), a 97% radiochemical yield of ^{18}F-**10a** was obtained (Fig. 4b). The specific activity of ^{18}F-**10** was determined to be 3.0 ± 1.0 Ci/μmol after purification by comparing the UV absorption with standard titration curve.

Cell Integrin Receptor-Binding Assay

Receptor-binding affinity studies of ^{19}F-**10** and unmodified c(RGDyK) toward $\alpha_v\beta_3$ integrin were performed using $\alpha_v\beta_3$ integrin–positive U87MG cells. Binding on the cell membrane allows cross-linking and integrin receptor multimerization, through which multivalent binding and clustering of receptor is studied in the natural context of the integrin. We compared the receptor-binding affinity of ^{19}F-**10** with that of unlabeled c(RGDyK) by performing competitive displacement studies with ^{125}I-echistatin (Fig. 3c). Both ^{19}F-**10** and unmodified c(RGDyK) peptides inhibited the binding of ^{125}I-echistatin to $\alpha_v\beta_3$ integrin–positive U87MG cells. The IC_{50} value for ^{19}F-**10** and c(RGDyK) was 39.8 ± 4.5 and 19.6 ± 3.2 nmol/L, respectively. Thus, the fluoride incorporation via tetrazine ligation into the cRGD peptide had minimal effect on binding affinity to the $\alpha_v\beta_3$ receptors.

In vivo Metabolism of ^{18}F-10

The metabolic stability of ^{18}F-**10** was determined in mouse blood, urine and in liver and kidney homogenates at 2 h after tracer injection. The extraction efficiency of all organs was between 56% and 98%. The lowest extraction efficiency was found for the kidney

homogenates and the highest extraction efficiency was from blood sample. The intact probes were 75%, 51%, 57%, and 62% for blood, kidney, liver, and urine samples respectively (Fig. 5). The major metabolites correlate well with the aromatized product. These results showed that the new probe displayed significantly higher stability than previous dipyridyl analogs.[27, 29]

microPET Studies

The localization of ^{18}F-**10** in human U87MG tumor-bearing nude mice (n = 5) was performed by multiple time-point static microPET scans. Figure 6a shows microPET images of a female mouse at different times after injection of 7.4 MBq (200 μCi) of ^{18}F-**10.** All microPET images were decay corrected. The tumor was clearly visualized with good contrast. Fig. 6b shows the microPET images with a blocking dose of unlabeled c(RGDyK) peptide coinjection. The tumor uptake of the radio probe was clearly reduced. The microPET imaging study demonstrated high and specific binding of ^{18}F-**10** to human U87MG tumors. Quantification of activity accumulation in the tumor and major organs (Fig. 6c) was determined by biodistribution studies conducted 2 h post injection.

DISCUSSION

Although dipyridyl-*s*-tetrazine conjugates with ^{18}F-**2** can be created rapidly and efficiently, in prior studies on RGD-based imaging[29] we observed that these conjugates have only moderate metabolic stability *in vivo*. We hypothesized that a conjugate with less electron withdrawing phenyl groups would be more stable, and in line with prior observations may spontaneously oxidize to give aromatic pyridazine products that are also highly stable.[5, 9] To test this hypothesis, we prepared the diphenyl-*s*-tetrazine derivatives **7** and **8** from precursor **6**. Compound **8** reacts with *trans*-cyclooctene derivative **9** in water/MeOH (6:4, v/v) at 25 °C with $k_2 = 1000 \pm 100\ M^{-1}\ s^{-1}$. When compared under similar conditions, the rate of reactivity for the CF_3-substitituted tetrazine **8** falls within an order of reactivity of the faster dipyridyl-*s*-tetrazine derivatives **3**.[6, 37]

Encouraged by the efficient reactivity of **8** with **9**, we reacted the cRGD-diphenyl-*s*-tetrazine derivative **7** with ^{19}F-**2** to provide conjugate **10a**, a mixture of isomers (Fig. 3a). In line with observations from model compounds,[36] we found that **10a** partially oxidized spontaneously in solution to provide aromatic **10b**. Shown in Fig. 3b is the HPLC–MS trace of the Diels-Alder conjugate from **7** (10 μM) and ^{19}F–**2** (10 μM) analyzed after standing overnight in aqueous solution. As expected,[5, 9] in addition to peaks from the dihydroaromatic Diels-Alder adducts **10a** (*m/z* 1176), we also observed the aromatized pyridizine adducts **10b** (*m/z* 1178). As shown in Fig. 3c, the receptor-binding affinity of **10** was compared to that of unlabeled c(RGDyK) by performing competitive displacement studies with ^{125}I-echistatin. The ^{19}F-cRGD conjugate **10** was comparable to the unlabeled cyclic RGD peptide in the ability to inhibit the binding of ^{125}I-echistatin to $\alpha_v\beta_3$ integrin–positive U87MG cells.

To study the stability of the ^{18}F-labeled Diels-Alder conjugates, an *in vivo* metabolic study was carried out by injecting ^{18}F-**10** into an athymic nude mouse that was sacrificed 2 h post injection. The organ uptake by the kidneys and liver for ^{18}F-**10** (Fig. 6) is similar to what

was observed with dipyridyl-*s*-tetrazine-RGD construct **4b** (Fig. 1c). As shown previously, the organ uptake was greatly reduced when the more hydrophilic probe **4a** based on the exendin-4 ligand (Fig. 1b) was used to image a GLP-1R positive tumor in mice.[30] Similarly, we anticipate that the pharmacokinetic/pharmacodynamic properties of probes related to **4a** will readily be improved with protein-based probes, or with peptide-based probes where hydrophilic spacer molecules are employed. For the present study to investigate the stability of the tetrazine-TCO conjugate *in vivo*, the organ uptake of ^{18}F-**10** was considered advantageous as it allowed study of probe that had been retained in these organs. Thus, major tissues were collected and homogenized, and the activity was extracted and analyzed by HPLC (Fig. 5). Fractions were collected each minute and radioactivity measured with the γ-counter. The average fraction of intact tracer was significantly improved relative to the first generation system **4b** (Fig. 1c), where only degradation products were observed by HPLC in similar attempts to recover radioactivity from blood, urine and organs of the animal. For ^{18}F-**10**, a hydrophilic byproduct was not observed by HPLC analysis, and the probe was detected with high fidelity in extracts from the kidneys, liver, blood and urine. To ensure that there was not a hydrophilic byproduct in the homogenates, we also analyzed the aqueous phase from the blood sample. The HPLC profile was very similar to that from the organic phase. In each of the metabolic extracts, two peaks were observed. Upon comparison of the HPLC data (Fig. 5) and LC/MS (Fig. 3b) data with cold conjugates it was concluded that one peak corresponded to the dihydropyridizine isomers of ^{18}F-**10a**, and the other peak to the aromatized isomers ^{18}F-**10b**. One limitation of using ^{18}F-**2** is the high number of isomeric conjugates that are formed upon conjugation with unsymmetrical tetrazines, which may present an issue for clinical translation. Efforts to ameliorate this issue by using higher symmetry cyclooctene derivatives are in progress.

^{18}F-**10** exhibited good metabolic stability *in vivo*, and injection of ^{18}F-**10** into a U87MG mouse model resulted in an effective method for $\alpha_v\beta_3$ imaging. The integrin $\alpha_v\beta_3$ receptor specificity was confirmed by blocking experiments, in which unlabeled cRGD was administered prior to the injection of the ^{18}F-**10** (Fig. 6). Thus, this labeling system has improved product stability, and no defluorination of ^{18}F-**10** was observed as no visible bone uptake was observed in any of the microPET scans. We also performed PBS stability study on newly synthesized ^{18}F-**10**. Around 28% of product got aromatized at 2 h post incubation (Fig S2).

A major advantage of the tetrazine ligation lies in the ability to enable fast reactivity at low micromolar concentrations within minutes and without an excess of either reactant. After demonstrating that the tetrazine **7** is robust and that conjugates with ^{18}F-**2** have good stability *in vivo*, we explored the lower limit of concentration for the ^{18}F labeling reaction. As benchmarks, the decay-corrected labeling yield was 35–45% when *N*-succinimidyl-4-^{18}F-fluorobenzoate was combined with an RGD derivative at 0.11 mM,[38] and 70% when an RGD derivative at 1.8 mM was labeled with ^{18}F by Cu-catalyzed azide/alkyne cycloaddition.[39] By contrast, the tetrazine–TCO ligation reaction is nearly quantitative at a concentration that is more dilute by more than 3 orders of magnitude (Fig. 4). Thus, a 97% radiochemical yield of ^{18}F-**10** was obtained in 5 minutes when ^{18}F-**2** (4 μCi/μL, 1 μM) was combined with only 4 equiv. of **7** (0.4 μg, 0.4nmol, 4 μM). We believe

that this combination of fast reactivity to yield metabolically stable conjugates should continue to enable applications in ^{18}F-based labeling and imaging.

CONCLUSION

A CF_3-substituted 3,6-diphenyl-*s*-tetrazine derivative displays fast conjugation rates toward ^{18}F-2, providing nearly quantitative ^{18}F labeling was observed within minutes at low micromolar concentrations. This bioorthogonal ligation reaction was used to construct an ^{18}F-cRGD conjugate, which was evaluated for integrin $\alpha_v\beta_3$ imaging in U87MG tumor-bearing mice by microPET. The conjugate was further shown to display improved metabolic stability in an *in vivo* mouse study.

ASSOCIATED CONTENT

Experimental procedures, spectral data for all new compounds, kinetic plots, and HPLC traces. This material is available free of charge via the Internet at http://pubs.acs.org.

MATERIALS AND METHODS

All commercially available chemical reagents were used without further purification. The syringe filter and polyethersulfone membranes (pore size, 0.22 μm; diameter, 13 mm) were obtained from Nalge Nunc International (Rochester, NY). ^{125}I-Echistatin was purchased from PerkinElmer (Piscataway, NJ). c(RGDyK) was obtained from Peptides International (Louisville, KY). All HPLC conditions are gradient. HPLC methods, NMR spectra and mass spectrometry details are listed in supplementary data. MicroPET scans were performed on a microPET R4 rodent model scanner (Siemens Medical Solutions USA, Inc., Knoxville, TN), or a GE eXplore Vista.

Chemistry

Detailed synthetic procedures and characterization details are provided as supporting material.

Stopped-flow kinetic analysis

The second order rate constant was measured under pseudo-first order conditions using an excess of TCO **9** by following the exponential decay of absorbance due to the tetrazine chromophore of **8** at 292 nm using an SX 18MV-R stopped-flow spectrophotometer (Applied Photophysics Ltd.). Thus, equal volumes of solutions of TCO **9** (0.50 mM, 1.0 mM or 2.0 mM in 60:40 water : methanol) and tetrazine **8** (0.050 mM in 60:40 water : methanol) were mixed in the stopped flow device. The final concentration of **8** was 25 μM, and **9** was 0.25 mM, 0.50 mM or 1.0 mM. At each concentration, kinetic data was repeated nine times (triplicate runs on three independent samples) at 298 K. Thus, 27 rate measurements were made. The rate constant was determined by nonlinear regression analysis using Prism (GraphPad Software, Inc.). The mean second order rate constant under these conditions was measured to be 1000 +/− 100 $M^{-1}s^{-1}$.

Radiochemistry

The ^{18}F-labeled TCO (^{18}F-**2**, Figure 1) was synthesized as reported.[27] A solution of 0.4 mCi (14.8 MBq) ^{18}F-**2** in ethanol was added to different concentrations of tetrazine-cRGD **7** in DMSO (total volume 100 μL). After vigorous vortexing for 1 min at room temperature, the reaction was quenched with 1 mL 0.1% TFA in water and loaded onto a C-18 HPLC column to determine the labeling yield. With a loading of **7** at 4μM, probe **10** was obtained with 97% labeling yield (Fig. 4). For small animal study, the HPLC fraction containing ^{18}F-**10** was collected and the HPLC eluent was removed using a rotary evaporator. ^{18}F-**10** was reconstituted in 1 mL PBS and passed through a 0.22 μm syringe filter for animal injection.

Cell Integrin Receptor-Binding Assay

In vitro integrin-binding affinities and specificities of tetrazine-cRGD peptides were assessed via displacement cell binding assays using ^{125}I-echistatin as the integrin-specific radioligand. Experiments were performed on the human glioblastoma U87MG cell line by modification of a method previously described.[31]

Animal Models

Animal procedures were performed according to a protocol approved by the UNC Institutional Animal Care and Use Committee. Human brain cancer carcinoma xenografts were induced by subcutaneous injection of 10^7 U87MG cells into the right front leg of female athymic nude mice. Three weeks after inoculation of the tumor cells, when the tumor reached 0.4–0.6 cm in diameter, the mice were used for microPET experiments.

Metabolic Stability

The metabolic stability of ^{18}F-**10** was evaluated in an athymic nude mouse bearing a U87MG tumor according a reported procedure.[32] Detailed procedures are included as supplementary material.

microPET Studies

PET of tumor-bearing mice was performed on an eXplore Vista microPET/CT rodent model scanner using a reported method.[33, 34] In brief, the mice were injected with 7.4 MBq of ^{18}F-RGD conjugate **10** with or without a blocking dose of unlabeled RGD peptide via the tail vein and then anesthetized with 2% isoflurane and placed near the center of the FOV of the microPET where the highest image resolution and sensitivity are obtained.

Supplementary Material

Refer to Web version on PubMed Central for supplementary material.

Acknowledgments

This work was supported by NIH Grant Number P20 RR017716 from the COBRE Program of the NCRR, NIBIB (7R01EB014354-02), P30CA014089, P30-CA016086-35-37 from the National Cancer Institute, and UNC Radiology Department and BRIC. Spectra were obtained with instrumentation supported by NSF CRIF:MU grants: CHE 0840401 and CHE-0541775.

References

1. Czernin J, Phelps ME. Positron emission tomography scanning: current and future applications. Annu Rev Med. 2002; 53:89–112. [PubMed: 11818465]
2. Gallagher BM, Fowler JS, Gutterson NI, MacGregor RR, Wan CN, Wolf AP. Metabolic trapping as a principle of radiopharmaceutical design: some factors resposible for the biodistribution of [^{18}F] 2-deoxy-2-fluoro-D-glucose. J Nucl Med. 1978; 19:1154–61. [PubMed: 214528]
3. Reivich M, Kuhl D, Wolf A, Greenberg J, Phelps M, Ido T, Casella V, Fowler J, Hoffman E, Alavi A, et al. The [^{18}F]fluorodeoxyglucose method for the measurement of local cerebral glucose utilization in man. Circ Res. 1979; 44:127–37. [PubMed: 363301]
4. Royzen M, Yap GP, Fox JM. A photochemical synthesis of functionalized *trans*-cyclooctenes driven by metal complexation. J Am Chem Soc. 2008; 130:3760–1. [PubMed: 18321114]
5. Blackman ML, Royzen M, Fox JM. Tetrazine ligation: fast bioconjugation based on inverse-electron-demand Diels-Alder reactivity. J Am Chem Soc. 2008; 130:13518–9. [PubMed: 18798613]
6. Lang K, Davis L, Wallace S, Mahesh M, Cox DJ, Blackman ML, Fox JM, Chin JW. Genetic Encoding of bicyclononynes and *trans*-cyclooctenes for site-specific protein labeling in vitro and in live mammalian cells via rapid fluorogenic Diels-Alder reactions. J Am Chem Soc. 2012; 134:10317–20. [PubMed: 22694658]
7. Rossin R, van den Bosch SM, Ten Hoeve W, Carvelli M, Versteegen RM, Lub J, Robillard MS. Highly reactive *trans*-cyclooctene tags with improved stability for Diels-Alder chemistry in living systems. Bioconjug Chem. 2013; 24:1210–7. [PubMed: 23725393]
8. Selvaraj R, Fox JM. *trans*-Cyclooctene--a stable, voracious dienophile for bioorthogonal labeling. Curr Opin Chem Biol. 2013; 17:753–60. [PubMed: 23978373]
9. Taylor MT, Blackman ML, Dmitrenko O, Fox JM. Design and synthesis of highly reactive dienophiles for the tetrazine-*trans*-cyclooctene ligation. J Am Chem Soc. 2011; 133:9646–9. [PubMed: 21599005]
10. Devaraj NK, Weissleder R, Hilderbrand SA. Tetrazine-based cycloadditions: application to pretargeted live cell imaging. Bioconjug Chem. 2008; 19:2297–9. [PubMed: 19053305]
11. Pipkorn R, Waldeck W, Didinger B, Koch M, Mueller G, Wiessler M, Braun K. Inverse-electron-demand Diels-Alder reaction as a highly efficient chemoselective ligation procedure: synthesis and function of a BioShuttle for temozolomide transport into prostate cancer cells. J Pept Sci. 2009; 15:235–41. [PubMed: 19177421]
12. Patterson DM, Nazarova LA, Xie B, Kamber DN, Prescher JA. Functionalized cyclopropenes as bioorthogonal chemical reporters. J Am Chem Soc. 2012; 134:18638–43. [PubMed: 23072583]
13. Yang J, Seckute J, Cole CM, Devaraj NK. Live-cell imaging of cyclopropene tags with fluorogenic tetrazine cycloadditions. Angew Chem Int Ed Engl. 2012; 51:7476–9. [PubMed: 22696426]
14. Chen W, Wang D, Dai C, Hamelberg D, Wang B. Clicking 1,2,4,5-tetrazine and cyclooctynes with tunable reaction rates. Chem Commun. 2012; 48:1736–8.
15. Karver MR, Weissleder R, Hilderbrand SA. Bioorthogonal reaction pairs enable simultaneous, selective, multi-target imaging. Angew Chem Int Ed Engl. 2012; 51:920–2. [PubMed: 22162316]
16. Niederwieser A, Spate AK, Nguyen LD, Jungst C, Reutter W, Wittmann V. Two-color glycan labeling of live cells by a combination of Diels-Alder and click chemistry. Angew Chem Int Ed Engl. 2013; 52:4265–8. [PubMed: 23468318]
17. Carroll L, Evans HL, Aboagye EO, Spivey AC. Bioorthogonal chemistry for pre-targeted molecular imaging--progress and prospects. Org Biomol Chem. 2013; 11:5772–81. [PubMed: 23907155]
18. Kettenbach K, Schieferstein H, Ross TL. ^{18}F-Labeling Using Click Cycloadditions. Biomed Res Int. 2014; 2014:361329. [PubMed: 25003110]
19. Reiner T, Zeglis BM. The inverse electron demand Diels-Alder click reaction in radiochemistry. J Labelled Comp Radiopharm. 2014; 57:285–90. [PubMed: 24347429]
20. Devaraj NK, Thurber GM, Keliher EJ, Marinelli B, Weissleder R. Reactive polymer enables efficient in vivo bioorthogonal chemistry. Proc Natl Acad Sci U S A. 2012; 109:4762–7. [PubMed: 22411831]

21. Devaraj NK, Upadhyay R, Haun JB, Hilderbrand SA, Weissleder R. Fast and sensitive pretargeted labeling of cancer cells through a tetrazine/*trans*-cyclooctene cycloaddition. Angew Chem Int Ed Engl. 2009; 48:7013–6. [PubMed: 19697389]
22. Rossin R, Lappchen T, van den Bosch SM, Laforest R, Robillard MS. Diels-Alder reaction for tumor pretargeting: in vivo chemistry can boost tumor radiation dose compared with directly labeled antibody. J Nucl Med. 2013; 54:1989–95. [PubMed: 24092936]
23. Rossin R, Verkerk PR, van den Bosch SM, Vulders RC, Verel I, Lub J, Robillard MS. In vivo chemistry for pretargeted tumor imaging in live mice. Angew Chem Int Ed Engl. 2010; 49:3375–8. [PubMed: 20391522]
24. Zeglis BM, Sevak KK, Reiner T, Mohindra P, Carlin SD, Zanzonico P, Weissleder R, Lewis JS. A pretargeted PET imaging strategy based on bioorthogonal Diels-Alder click chemistry. J Nucl Med. 2013; 54:1389–96. [PubMed: 23708196]
25. Denk C, Svatunek D, Filip T, Wanek T, Lumpi D, Frohlich J, Kuntner C, Mikula H. Development of a ^{18}F-Labeled Tetrazine with Favorable Pharmacokinetics for Bioorthogonal PET Imaging. Angew Chem Int Ed Engl. 2014; 53:9655–9. [PubMed: 24989029]
26. Herth MM, Andersen VL, Lehel S, Madsen J, Knudsen GM, Kristensen JL. Development of a ^{11}C-labeled tetrazine for rapid tetrazine-*trans*-cyclooctene ligation. Chem Commun. 2013; 49:3805–7.
27. Li Z, Cai H, Hassink M, Blackman ML, Brown RC, Conti PS, Fox JM. Tetrazine-*trans*-cyclooctene ligation for the rapid construction of ^{18}F labeled probes. Chem Commun. 2010; 46:8043–5.
28. Liu S, Hassink M, Selvaraj R, Yap LP, Park R, Wang H, Chen X, Fox JM, Li Z, Conti PS. Efficient ^{18}F labeling of cysteine-containing peptides and proteins using tetrazine-*trans*-cyclooctene ligation. Mol Imaging. 2013; 12:121–8. [PubMed: 23415400]
29. Selvaraj R, Liu S, Hassink M, Huang CW, Yap LP, Park R, Fox JM, Li Z, Conti PS. Tetrazine-*trans*-cyclooctene ligation for the rapid construction of integrin $\alpha_v\beta_3$ targeted PET tracer based on a cyclic RGD peptide. Bioorg Med Chem Lett. 2011; 21:5011–4. [PubMed: 21601452]
30. Wu Z, Liu S, Hassink M, Nair I, Park R, Li L, Todorov I, Fox JM, Li Z, Shively JE, et al. Development and evaluation of ^{18}F-TTCO-Cys40-Exendin-4: a PET probe for imaging transplanted islets. J Nucl Med. 2013; 54:244–51. [PubMed: 23297075]
31. Chen X, Sievers E, Hou Y, Park R, Tohme M, Bart R, Bremner R, Bading JR, Conti PS. Integrin $\alpha_v\beta_3$-targeted imaging of lung cancer. Neoplasia. 2005; 7:271–9. [PubMed: 15799827]
32. Liu S, Li Z, Yap LP, Huang CW, Park R, Conti PS. Efficient preparation and biological evaluation of a novel multivalency bifunctional chelator for ^{64}Cu radiopharmaceuticals. Chem Eur j. 2011; 17:10222–5. [PubMed: 21815227]
33. Liu S, Li D, Park R, Liu R, Xia Z, Guo J, Krasnoperov V, Gill PS, Li Z, Shan H, et al. PET imaging of colorectal and breast cancer by targeting EphB4 receptor with ^{64}Cu-labeled hAb47 and hAb131 antibodies. J Nucl Med. 2013; 54:1094–100. [PubMed: 23667241]
34. Liu S, Li D, Shan H, Gabbai FP, Li Z, Conti PS. Evaluation of ^{18}F-labeled BODIPY dye as potential PET agents for myocardial perfusion imaging. Nucl Med Biol. 2014; 41:120–6. [PubMed: 24210284]
35. Liu DS, Tangpeerachaikul A, Selvaraj R, Taylor MT, Fox JM, Ting AY. Diels-Alder cycloaddition for fluorophore targeting to specific proteins inside living cells. J Am Chem Soc. 2012; 134:792–795. [PubMed: 22176354]
36. In a model study, the N-acetyl derivative of 6 was reacted with trans-cyclooctene. The initially formed dihydropyridazine product partially oxidized to the pyridazine on workup. After separation by column chromatography, the pyridazine could be isolated in pure form, but the dihydropyridazine product continued to slowly oxidize upon dissolution.
37. The rate of reaction for a derivative of dipyridyltetrazine 3 with the equatorial diastereomer of 5-hydroxy-*trans*-cyclooctene is k_2 5280 $M^{-1}s^{-1}$ at 25 °C in 55:45 water:MeOH. See ref 6.
38. Chen X, Park R, Shahinian AH, Tohme M, Khankaldyyan V, Bozorgzadeh MH, Bading JR, Moats R, Laug WE, Conti PS. ^{18}F-labeled RGD peptide: initial evaluation for imaging brain tumor angiogenesis. Nucl Med Biol. 2004; 31:179–89. [PubMed: 15013483]

39. Li ZB, Wu Z, Chen K, Chin FT, Chen X. Click chemistry for ^{18}F-labeling of RGD peptides and microPET imaging of tumor integrin $\alpha_v\beta_3$ expression. Bioconjug Chem. 2007; 18:1987–94. [PubMed: 18030991]

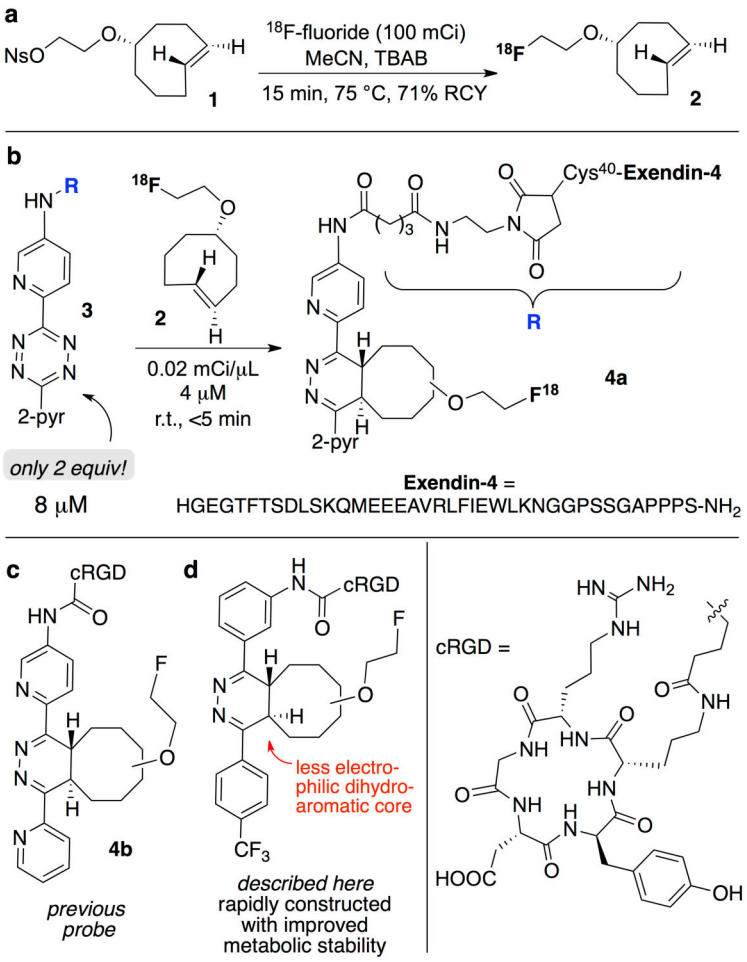

Figure 1.

(a) Synthesis of ^{18}F-TCO **2**. (b) Rapid ^{18}F-labeling of a 4.8 kDa peptide takes place rapidly at low concentration using only a 2-fold excess of the peptide precursor. (c) Probe **4b** has been used to image U87MG tumors in mice. (d) A new probe that can also be constructed rapidly and used for U87MG tumor imaging in mice with the added benefit of improved metabolic stability.

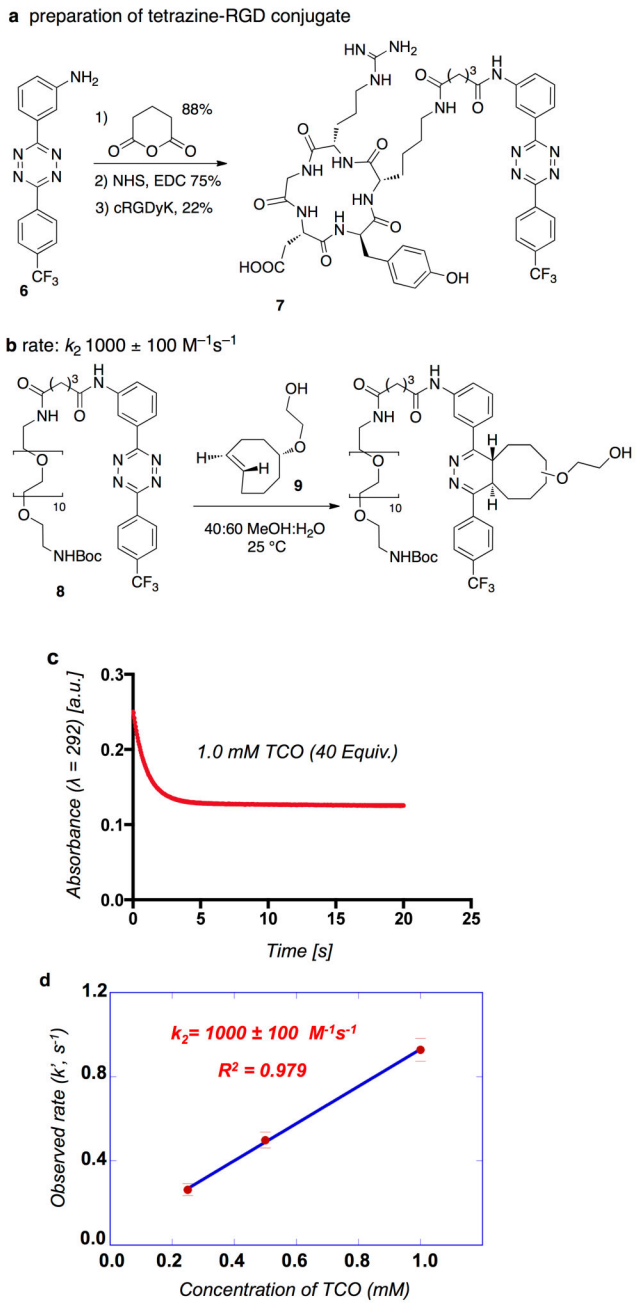

Figure 2.

(a) Synthesis of a cRGD-diphenyl-*s*-tetrazine conjugate. (b) The rate of the conjugation of **8** with **9** was determined by stopped-flow kinetic analysis. (c) The exponential plot of the reaction of **8** (25 μM) and **9** (1.0 mM) in 40:60 MeOH:water was monitored at 292 nm. Data was recorded for 20 s at 298 K, with triplicate runs on three independent samples at three different concentrations (27 runs total). (d) The average of three observed rates k' vs concentration of **9** for the reaction between **8** and **9.** Under these pseudo-first order conditions the second order rate constant (k_2) was determined by nonlinear regression to be 1000 +/− 100 $M^{-1}s^{-1}$.

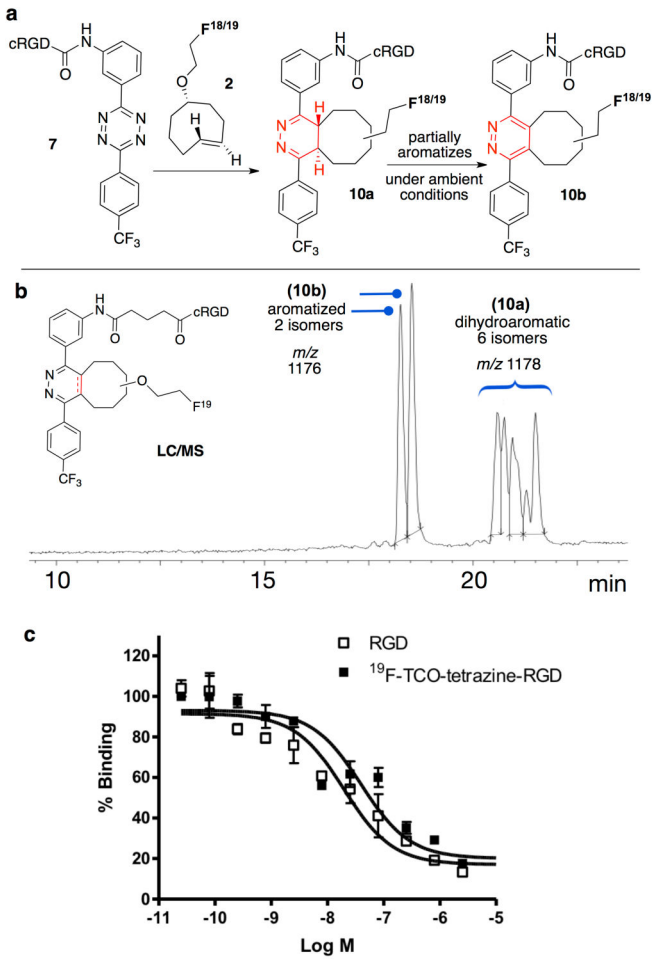

Figure 3.

(a) Conjugation of a cyclic-RGD-tetrazine **7** with F-TCO **2** gives conjugates **10a**, which slowly oxidize to aromatic isomers **10b** under ambient conditions in aqueous solution. (b) LC/MS analysis of the Diels-Alder conjugate from ^{19}F–**2** acquired after the sample had been allowed to stand overnight shows a mixture of aromatized and more slowly eluting dihydroaromatic products. Chromatographic resolution was higher and retention times longer in this LC/MS run than in radio-HPLC analyses (Fig 4, 5). (c) Cell-binding assay of c(RGDyK) and ^{19}F-Diels-Alder conjugates **10** using U87MG cells (integrin $\alpha_v\beta_3$-positive human glioblastoma). The cell-binding affinity of the peptides was determined by performing competitive displacement studies with ^{125}I-echistatin (n = 3).

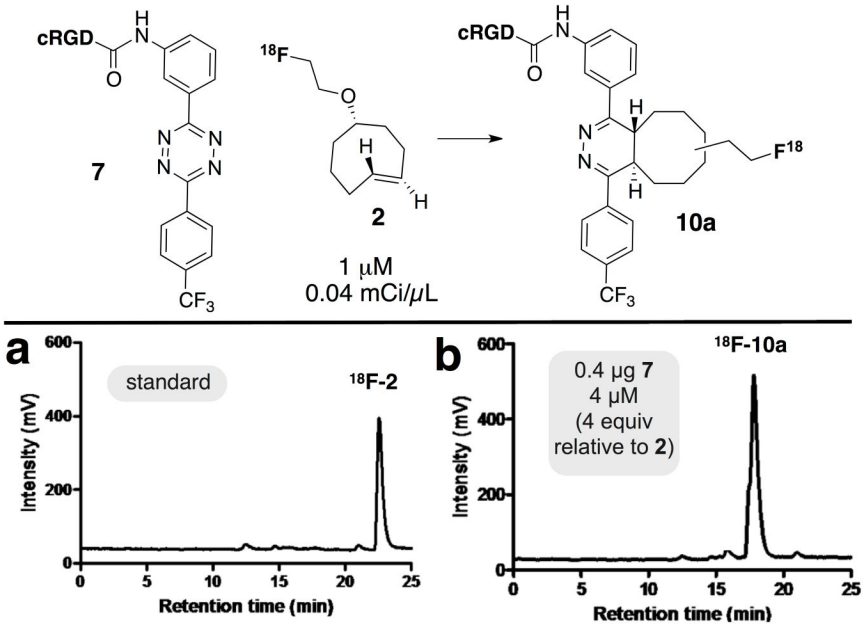

Figure 4.

^{18}F labeling by ^{18}F-**2** (1 μM) with differing concentrations of **7**. The product ^{18}F-**10a** is a mixture of regioisomers. (a) HPLC standard of ^{18}F-**2**. (b) 97% radiochemical yield with 4 equiv of **2**. The specific activity of ^{18}F-**10** was determined to be 3.0 ± 1.0 Ci/μmol after purification by comparing the UV absorption with standard titration curve.

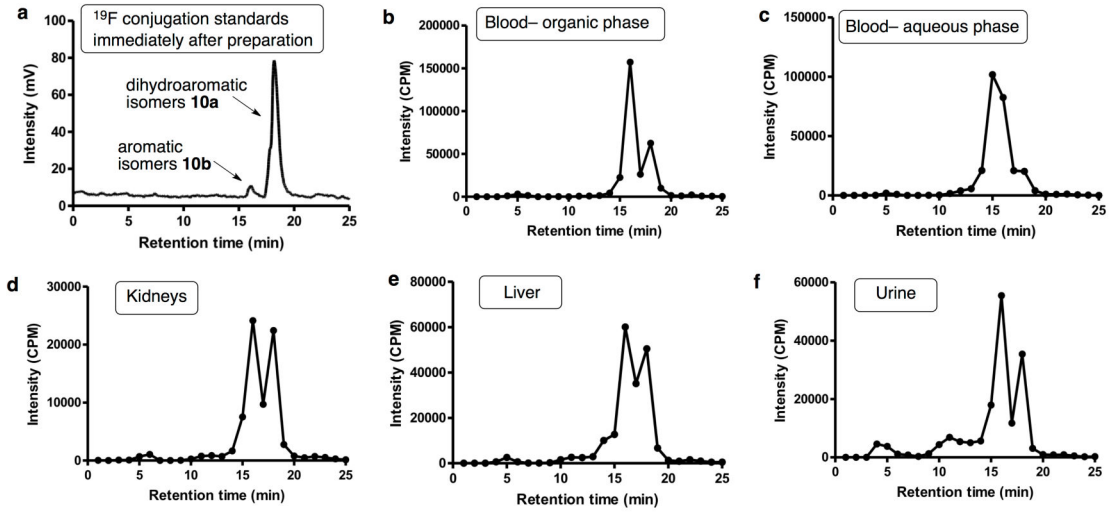

Figure 5.

Metabolic stability of ^{18}F-**10** in mouse blood and urine samples and in liver, and kidney homogenates at 1 h after injection. Fractions were collected every minute and radioactivity measured by γ-counter. The radio-HPLC profile of ^{18}F-**10** standard is also shown. In each of the metabolic extracts, two peaks were observed. One peak corresponded to dihydropyridizine isomers ^{18}F-**10a,** the other peak corresponded to isomers of pyridizine ^{18}F-**10b.**

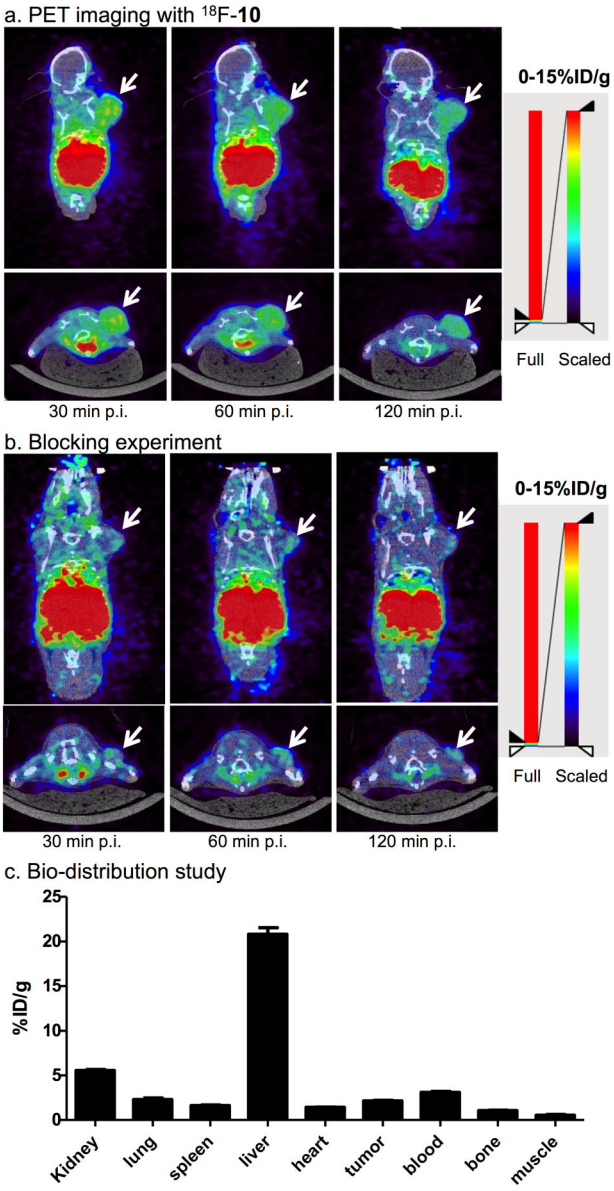

Figure 6.

microPET images of athymic nude mice bearing U87MG tumor at 0.5, 1, and 2 h after injection of ^{18}F-**10** (a) without or (b) with a blocking dose of *c*(RGDyK) peptide (10 mg/kg body weight) (n = 5). Tumors are indicated by arrows. (c) bio-distribution study of ^{18}F-**10** in nude mice bearing U87MG tumor at 2 h p.i..